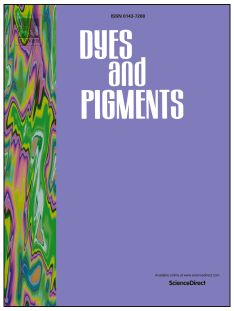

Optically operated second order optical effects in some substituted 4-(5-nitro-1,3-benzoxazol-2-yl)aniline chromophores

P. Szlachcic, A.A. Fedorchuk, A. Danel, B. Jarosz, A.M. El Naggar, A.A. Albassam, A. Wojciechowski, E. Gondek, T. Uchacz, K. Stadnicka, G. Lakshminarayana, I.V. Kityk

PII: S0143-7208(16)30843-9

DOI: 10.1016/j.dyepig.2017.02.009

Reference: DYPI 5786

To appear in: *Dyes and Pigments*

Received Date: 27 September 2016

Revised Date: 6 February 2017

Accepted Date: 7 February 2017

Please cite this article as: Szlachcic P, Fedorchuk AA, Danel A, Jarosz B, El Naggar AM, Albassam AA, Wojciechowski A, Gondek E, Uchacz T, Stadnicka K, Lakshminarayana G, Kityk IV, Optically operated second order optical effects in some substituted 4-(5-nitro-1,3-benzoxazol-2-yl)aniline chromophores, *Dyes and Pigments* (2017), doi: 10.1016/j.dyepig.2017.02.009.

Graphical abstract

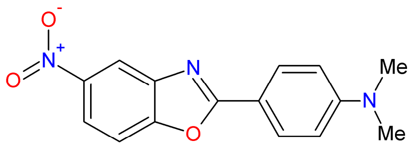

DMA

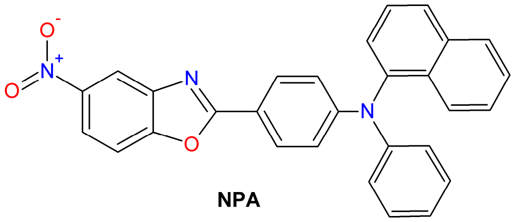

NPA

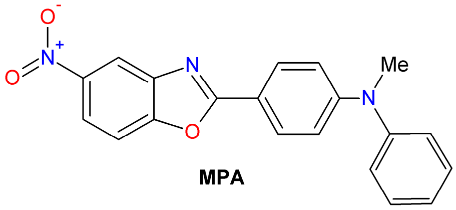

MPA

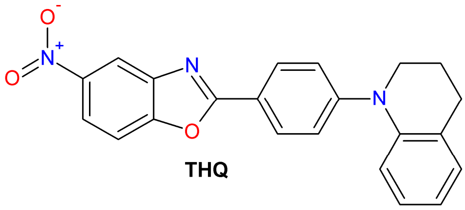

THQ

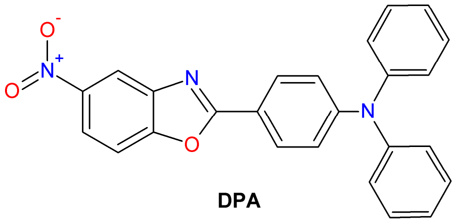

DPA

Optically operated second order optical effects in some substituted 4-(5-nitro-1,3-benzoxazol-2-yl)aniline chromophores

P. Szlachcic[1,*], A.A. Fedorchuk[2], A. Danel[1], B. Jarosz[1], A.M. El Naggar[3,4], A.A. Albassam[3], A.Wojciechowski[5], E. Gondek[6], T. Uchacz[7], K. Stadnicka[7], G. Lakshminarayana[8,*], I.V. Kityk[5]

[1] Institute of Chemistry, Faculty of Food Technology, Agricultural University,
ul. Balicka 122, 31-149 Kraków, Poland
[2] Ivan Franko National University of Lviv, Faculty of Chemistry,
Kyryla I Mefodiya, 6, Lviv, 79005, Ukraine
[3] Research Chair of Exploitation of Renewable Energy Applications in Saudi Arabia, Physics and Astronomy Department, College of Science,
King Saud University, P.O. Box 2455, Riyadh 11451, Saudi Arabia
[4] Physics Department, Faculty of Science, Ain Sham University,
Abbasia, Cairo 11566, Saudi Arabia
[5] Faculty of Electrical Engineering, Częstochowa University Technology,
ul. Armii Krajowej 17, PL-42-201 Częstochowa, Poland
[6] Institute of Physics, Technical University of Kraków,
ul. Podchorążych 1, 30-084 Kraków, Poland
[7] Faculty of Chemistry, Jagiellonian University,
ul. Ingardena 3, 30-060 Kraków, Poland
[8] Wireless and Photonic Networks Research Centre, Faculty of Engineering, Universiti Putra Malaysia,43400 Serdang, Selangor, Malaysia

Abstract

In this work, we report on second order nonlinear optical (NLO) susceptibilities of some substituted 4-(5-nitro-1,3-benzoxazol-2-yl)aniline chromophores that were embedded into photopolymer matrices. Depending on the photo-induced nitrogen laser (wavelength 371 nm) power density of photo-solidification we found an optimal photo-solidification parameter to achieve maximum second harmonic generation (SHG). The influence of the π-conjugated bonds on the output second order susceptibility and HOMO-LUMO level positions is analysed. The performed experiments are compared with the theoretically calculated microscopic hyper-polarizabilities obtained within the B3LYP DFT approach. The possible operation by the output SHG efficiency versus the photoinduced laser power density is presented. The role of the intra-molecular and surrounding polymers in the observed nonlinear optical behaviour is explored.

***Keywords*:**
second order optical chromophore;
photo-solidification;
benzoxazole;
DFT simulations;
X-ray diffraction

* Corresponding authors: G. Lakshminarayana (E-mail: glnphysics@gmail.com)
Tel: +60-89466438
P. Szlachcic (E-mail: p.szlachcic@ur.krakow.pl)
Tel: +48-126624054

1. Introduction

Recently, one can observe an enhanced interest in the search of organic chromophores, which possess second-order optical effects for their application in second-order nonlinear optics (NLO) [1–11] and in laser modulators, deflectors, telecommunications and optical information processes [12–14]. Such materials are developed in different directions: modification of π-conjugated bonds, addition of highly polarized backside groups, and formation of d-π metal–ligand charge transfer complexes [15–18]. General theory on the phenomenological and microscopic levels was developed in Refs. [19–26]. Main efforts were devoted for achieving the higher order hyper-polarizabilities [27, 28]. A flexible approach describing the possible ways for enhancement of the second order susceptibilities near the resonance and off-resonance cases was proposed recently [29, 30]. For this approach two principal parameters are proposed to utilize – the energy of the transition from the ground to the first excited states, and the second one – the number of effective conjugated electrons.

This article presents further development of this approach by incorporation of the small size organic NLO chromophores into the photopolymer matrices. By varying the power of photo-solidifying UV laser, it was shown a possibility of operation by second-order nonlinear optical constants using external photo-solidifying laser field with assistance of dc-electric aligned field. As a consequence, macroscopic susceptibility will be field oriented. All the earlier works usually neglected this influence.

As a chromophore for the NLO effects, we have applied novel nitro-benzoxazole derivatives presenting the non-symmetric chromophores which can be applied for nonlinear optics of chromophores with relatively small size. Benzoxazole-derivatives have been already studied for their NLO effects, but most of these researches were done on the polymers containing benzoxazole moiety in the side chain [31–37]. Non-polymeric derivatives have been also studied, but till now only the molecules with different substituent architecture, when compared to our research, were used [38–46]. Small and simple donor-acceptor molecules investigated in this work have not been studied yet, and the observed results could be used as a reference for longer, differently substituted benzoxazole molecules. Benzoxazole-derivatives proposed in the present work had been preliminarily studied for their NLO effects in powder form, however the obtained efficiency was low (about 0.8 pm/V for λ=1064 nm). Their interactions with the polymer matrix will be more efficient due to possible superposition of the external fields. During the UV photo-solidification between the chromophore and surrounding polymer matrix there remains some small liquid (non-solidified sheets on the borders of photopolymer-chromophore) which allows orienting spatially particular chromophore by external fields as described previously [47,48]. We also performed the DFT simulations of molecular hyper-polarizabilities of the synthesized compounds, in order to compare with the measured second harmonic generation (SHG). The origin of the nonlinear optical effects is discussed with respect to the space distribution of the particular HOMO and LUMO levels as well as energy magnitudes of their levels.

2. Experimental

2.1. General considerations

All the solvents used for the reactions and purifications were purchased from Dorchem (Polish supplier), and were of analytical grade. Dichloromethane used for spectroscopic and electrochemical studies was of spectrophotometric grade (Alpha Aesar). Silica Gel 60 and Aluminium Oxide 90 for a column chromatography were purchased from Merck. Polyphosphoric acid, 4-nitro-2-aminophenol, 2-aminophenol, benzoic acid, 4-bromobenzoic acid, *N*,*N*-dimethyl-4-aminobenzoic acid, diphenylamine, *N*-methylaniline, 1,2,3,4-tetrahydroquinoline, (1-naphtyl)phenylamine, sodium *tert*-butylate, (2-biphenyl)di-*tert*-butylphosphine, tetrabutylammonium hexafluorophosphate, ferrocene and Pd_2dba_3 were purchased from Alfa Aesar or Aldrich and used without further purification. $CDCl_3$ with TMS was purchased from Aldrich. Melting points were measured on an MEL-TEMP II apparatus and they are uncorrected. ^{1}H NMR and ^{13}C NMR were recorded at 600 MHz and 150 MHz, respectively, with a Bruker Avance III 600 spectrometer using $CDCl_3$ as a solvent. The chemical shifts were given in ppm (δ) from TMS as an internal standard. Elemental analyses were conducted at Elementar Vario MICRO cube. Diffraction data were collected for single crystals either with an Agilent Technologies SuperNova™ diffractometer, (low-temperature Cryo-Jet device, Atlas CCD detector) [49], using Mo Kα radiation (except of **D_RT** which was measured using Cu Kα radiation) or with the Nonius KappaCCD diffractometer using graphite monochromated Mo Kα radiation (data collection: COLLECT [50], cell refinement: HKL SCALEPACK [51], data reduction: HKL DENZO and SCALEPACK [51]). Cyclic voltammetry (CV) measurements were carried out on a PalmSens3 potentiostat. One platinum wire (ø = 0.5 mm) and platinum coil (ø = 1.6 mm) were used as a counter and working electrodes, respectively. Non aqueous electrode (Ag/Ag^+) designed and provided by ALS was used as a quasi-reference electrode. The potential of quasi-reference electrode was calibrated using the ferrocene as an internal standard. The solutions of compounds under the study ($\sim 5 \cdot 10^{-4}$ M) were prepared in suitable electrolyte ($\sim 1 \cdot 10^{-1}$ M solution of $Bu_4N^+PF_6^-$ in dichloromethane), the measurements were conducted at room temperature with the scan rate of 100 mV/s. Prior to the measurements, the solutions were purged with argon to remove residual oxygen. The dyes concentration used for spectroscopic measurements amounted to ca. $5 \cdot 10^{-6}$ M. UV-Vis. electronic absorption spectra in dichloromethane were recorded using a Shimadzu UV-2101 PC spectrometer.

2.2. Synthetic procedures and NMR spectroscopy

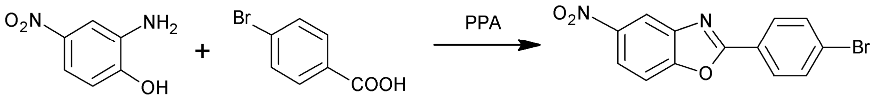

2.2.1. 2-(4-Bromophenyl)-5-nitro-1,3-benzoxazole: 4-nitro-2-aminophenol (50 mmol) and 4-bromobenzoic acid (50 mmol) were mixed with polyphosphoric acid (100 g). The reaction mixture was magnetically stirred for 24 hours at 110 °C (the flask was stopped with anhydrous calcium chloride tube) applying known procedure [52]. Then the reaction mixture was poured into ice-water and formed a waxy precipitate. After being neutralized with Na_2CO_3, the precipitate formed a light-brown powder, which was filtered off, washed with water and dried in air. Crude product was dissolved in $CHCl_3$ and flashed through aluminium oxide. The obtained yellowish powder was pure enough for the next steps, 8.59 g (54%). Small sample was recrystallized from toluene, light-yellow needles, m.p. 248-249°C. ^{1}H NMR (600 MHz, $CDCl_3$): δ = 8.66 (d, *J* = 2.2 Hz, 1H), 8.34 (dd, *J* = 8.9, 2.3 Hz, 1H), 8.13-8.15 (m, 2H), 7.71-7.73 (m, 2H), 7.69 (d, *J* = 8.9 Hz, 1H). ^{13}C NMR (150 MHz, $CDCl_3$): δ = 165.1, 154.2, 145.6, 142.5, 132.5, 129.4, 127.6, 124.9, 121.4, 116.4, 110.8. *Anal.* Calcd. for $C_{13}H_7BrN_2O_3$: C 48.93, H 2.21, N 8.78. Found: C 48.60, H 2.19, N 9.01.

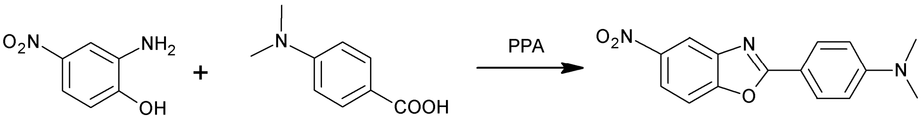

*2.2.2. N,N-Dimethyl-4-(5-nitro-1,3-benzoxazol-2-yl)aniline (**DMA**)*: 4-nitro-2-aminophenol (10 mmol) and *N,N*-dimethyl-4-aminobenzoic acid (11 mmol) were mixed with polyphosphoric acid (20 g). The reaction mixture was magnetically stirred for 24 hours at 110 °C (the flask was stopped with anhydrous calcium chloride tube). Then the reaction mixture was poured into ice-water. A precipitate was filtered off, washed with water and dried in air. Crude product was crystallised twice from DMF. Yellow-golden plates, 1.35 g (48%), m.p. 247-248 °C. ^{1}H NMR (600 MHz, $CDCl_3$): δ = 8.53 (d, *J* = 2.2 Hz, 1H), 8.22 (dd, *J* = 8.8, 2.3 Hz, 1H), 8.08-8.11 (m, 2H), 7.57 (d, *J* = 8.8 Hz, 1H), 6.76-6.78 (m, 2H), 3.10 (s, 6H). ^{13}C NMR (150 MHz, $CDCl_3$): δ = 167.2, 154.3, 153.0, 145.2, 143.3, 129.6, 120.0, 115.0, 112.6, 111.5, 109.9, 40.1. *Anal.* Calcd. for $C_{15}H_{13}N_3O_3$: C 63.60, H 4.63, N 14.83. Found: C 63.82, H 4.52, N 14.78.

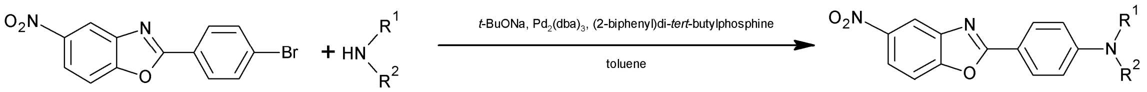

*2.2.3. General procedure for the synthesis of N-methyl-4-(5-nitro-1,3-benzoxazol-2-yl)-N-phenylaniline (**MPA**), 4-(5-nitro-1,3-benzoxazol-2-yl)-N,N-diphenylaniline (**DPA**), N-(1-naphtyl)-4-(5-nitro-1,3-benzoxazol-2-yl)-N-phenylaniline (**NPA**) and 1-[4-(5-nitro-1,3-benzoxazol-2-yl)phenyl]-1,2,3,4-tetrahydroquinoline (**THQ**)*:

638 mg (2 mmol) of 2-(4-bromophenyl)-5-nitro-1,3-benzoxazole was dissolved in 15 ml of toluene (dried over molecular sieves 4A). Toluene was deoxygenated before use by purging with dry argon. Then 269 mg (2.8 mmol) of sodium *tert*-butylate was added, followed by 37 mg (2 mol %) of $Pd_2(dba)_3$ and 30 mg (5 mol%) of (2-biphenyl)di-*tert*-butylphosphine, applying known procedure [53]. As the last, 2.4 mmol of corresponding amine was added; the flask was stopped with septa and the reaction mixture was stirred at ambient temperature under argon atmosphere for 48 h. After that, the reaction mixture was filtered; a precipitate was washed with toluene. The solvent was removed under reduced pressure; the residue was dissolved in $CHCl_3$ and flashed over Aluminium Oxide. The solution was then concentrated and the product was adsorbed on Silica Gel 60 and the solvent was removed. A dry adsorbent was put on the Silica Gel 60 column and eluted with toluene / petroleum ether (1:1) mixture. Resulted yellow solid was crystallized from toluene.

*2.2.3.1. N-Methyl-4-(5-nitro-1,3-benzoxazol-2-yl)-N-phenylaniline (**MPA**)*: *N*-methylaniline was used as an amine. In this case, the reaction was quenched with water, and the product was extracted with ethyl acetate. The extract was dried over anhydrous $MgSO_4$ and flashed through aluminium oxide. Crude product was purified according to the general procedure to give 453 mg (66 %) of an yellow powder, m.p. 185-188 °C. ^1H NMR (600 MHz, $CDCl_3$): δ = 8.54 (d, J = 2.2 Hz, 1H), 8.24 (dd, J = 8.8, 2.2 Hz, 1H), 8.04-8.06 (m, 2H), 7.59 (d, J = 8.8 Hz, 1H), 7.42-7.45 (m, 2H), 7.25-7.27 (m, 3H), 6.86-6.88 (m, 2H), 3.42 (s, 3H). ^{13}C NMR (150 MHz, $CDCl_3$): δ = 166.8, 154.3, 152.3, 147.1, 145.2, 143.1, 129.9, 129.4, 126.2, 125.8, 120.2, 115.2, 114.5, 114.3, 110.1, 40.3. *Anal.* Calcd. for $C_{20}H_{15}N_3O_3$: C 69.56, H 4.38, N 12.17. Found: C 69.40, H 4.25, N 12.20.

*2.2.3.2. 4-(5-Nitro-1,3-benzoxazol-2-yl)-N,N-diphenylaniline (**DPA**)*: diphenylamine was used as an amine following the general procedure to give 314 mg (39 %) of yellow plates, m.p. 199-201 °C. ^1H NMR (600 MHz, $CDCl_3$): δ = 8.57 (d, J = 2.2 Hz, 1H), 8.26 (dd, J = 8.9, 2.3 Hz, 1H), 8.04-8.06 (m, 2H), 7.61 (d, J = 8.9 Hz, 1H), 7.33-7.36 (m, 4H), 7.15-7.20 (m, 6H), 7.09-7.11 (m, 2H). ^{13}C NMR (150 MHz, $CDCl_3$): δ = 166.2, 154.3, 151.8, 146.4, 145.3, 143.0, 129.7, 129.2, 126.0, 124.8, 120.5, 120.4, 117.5, 115.6, 110.3. *Anal.* Calcd. for $C_{25}H_{17}N_3O_3$: C 73.70, H 4.21, N 10.31. Found: C 73.56, H 4.06, N 10.28.

*2.2.3.3. N-(Napht-1-yl)-4-(5-nitro-1,3-benzoxazol-2-yl)-N-phenylaniline (**NPA**):* (1-naphtyl)phenylamine was used as an amine following the general procedure to give 202 mg (22%) of an yellow powder, m.p. 206-208°C. ^1H NMR (600 MHz, $CDCl_3$): δ = 8.55 (d, J = 2.2 Hz, 1H), 8.23

(dd, J = 8.9, 2.3 Hz, 1H), 7.99-8.02 (m, 2H), 7.92 (d, J = 8.3 Hz, 1H), 7.90 (d, J = 8.6 Hz, 1H), 7.85 (d, J = 8.3 Hz, 1H), 7.57 (d, J = 8.9 Hz, 1H), 7.48-7.53 (m, 2H), 7.39-7.41 (m, 2H), 7.29-7.32 (m, 2H), 7.23-7.25 (m, 2H), 7.09-7.12 (m, 1H), 6.96-6.98 (m, 2H). ^{13}C NMR (150 MHz, CDCl$_3$): δ = 166.3, 154.3, 152.3, 146.5, 145.3, 143.0, 142.0, 135.3, 130.9, 129.6, 129.3, 128.6, 127.6, 127.5, 126.9, 126.5, 126.4, 124.4, 124.3, 123.7, 120.4, 118.6, 116.8, 115.5, 110.2. *Anal.* Calcd. for $C_{29}H_{19}N_3O_3$: C 76.14, H 4.19, N 9.19. Found: C 76.20, H 4.15, N 9.10.

*2.2.3.4. 1-[4-(5-nitro-1,3-benzoxazol-2-yl)phenyl]-1,2,3,4-tetrahydroquinoline (**THQ**):* 1,2,3,4-tetrahydroquinoline was used as an amine following the general procedure to give 155 mg (21%) of light-orange plates, m.p. 189-190 (dec.)°C. ^{1}H NMR (600 MHz, CDCl$_3$): δ = 8.58 (d, J = 2.2 Hz, 1H), 8.27 (d, J = 8.8, 2.3 Hz, 1H), 8.12-8.14 (m, 2H), 7.62 (d, J = 8.9 Hz, 1H), 7.31-7.33 (m, 2H), 7.20 (d, J = 8.1 Hz, 1H), 7.14 (br d, J = 7.5 Hz, 1H), 7.06-7.09 (m, 1 H), 6.91 (td, J = 7.4, 1.2 Hz, 1H), 3.73 (t, J = 6.1 Hz, 2H), 2.80 (t, J = 6.4 Hz, 2H), 2.05 (quintet, J = 6.2 Hz, 2H). ^{13}C NMR (150 MHz, CDCl$_3$): δ = 166.3, 154.3, 151.8, 145.3, 143.0, 141.6, 129.29, 129.26, 129.22, 126.4, 121.6, 120.5, 119.8, 119.4, 117.5, 115.6, 110.3, 49.1, 27.4, 23.7. *Anal.* Calcd. for $C_{22}H_{17}N_3O_3$: C 71.15, H 4.61, N 11.31. Found: C 71.01, H 4.52, N 11.35.

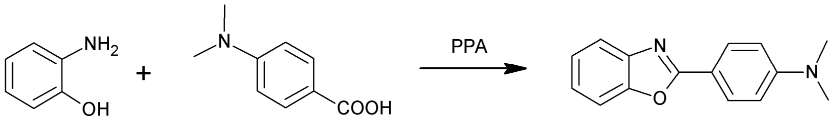

*2.2.4. N,N-Dimethyl-4-(1,3-benzoxazol-2-yl)aniline (**D**)*: 2-aminophenol (25 mmol) and *N,N*-dimethyl-4-aminobenzoic acid (25 mmol) were mixed with polyphosphoric acid (50 g). The reaction mixture was magnetically stirred for 24 hours at 110 °C (the flask was stopped with anhydrous calcium chloride tube). Then the reaction mixture was poured into ice-water. Precipitate was filtered off, washed with Na_2CO_3 solution and water and dried in air. Crude product was crystallized ten times from toluene. Colourless plates, 3.50 g (59%), m.p. 185-187 °C (Lit. 182.3-183.7 °C [54]). ^{1}H NMR and ^{13}C NMR match those found earlier [54]. *Anal.* Calcd. for $C_{15}H_{14}N_2O$: C 75.61, H 5.92, N 11.76. Found: C 75.70, H 5.90, N 11.78.

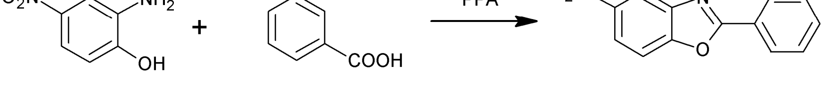

*2.2.5. 2-Phenyl-5-nitro-1,3-benzoxazole (**A**)*: That compound was prepared according to a known procedure from 10 mmol of 4-nitro-2-aminophenol and benzoic acid [55]. Colourless plates, 1.34 g (56%), m.p. 174-175 °C (Lit. 177 °C [56]). ^{1}H NMR and ^{13}C NMR match those found earlier [56]. *Anal.* Calcd. for $C_{13}H_8N_2O_3$: C 65.00, H 3.36, N 11.66. Found: C 65.28, H 3.35, N 11.50.

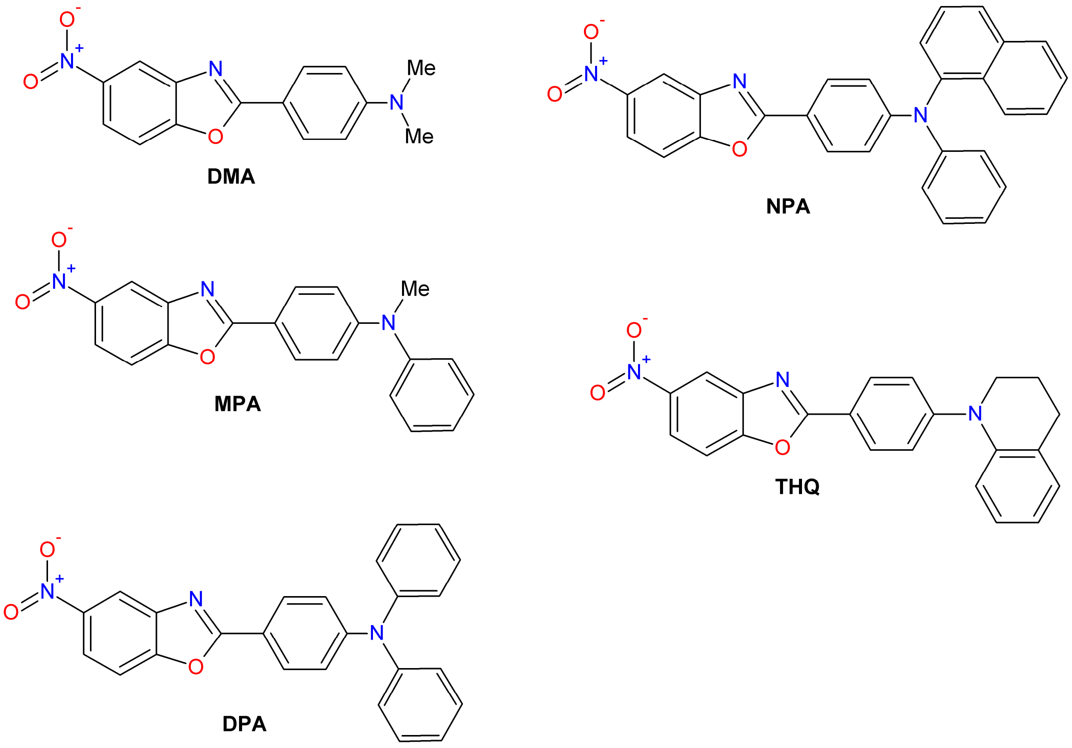

Fig. 1. General molecular formula of the studied chromophores

3. Results and discussion

3.1. X-ray crystallography

Crystal structure studies were performed for **DMA** (Fig. 2 (1)), **DPA** (Fig. 2 (2)) and **THQ** (Fig. 2 (3)) derivatives and for reference compounds: 2-phenyl-5-nitro-1,3-benzoxazole (acceptor-group-only) **A** (Fig. 2 (4) and *N*,*N*-imethyl-4-(1,3-benzoxazol-2-yl)aniline (donor-group-only) **D** (Fig. 2 (5)). All studied crystals were obtained by slow cooling of hot and saturated toluene solutions.

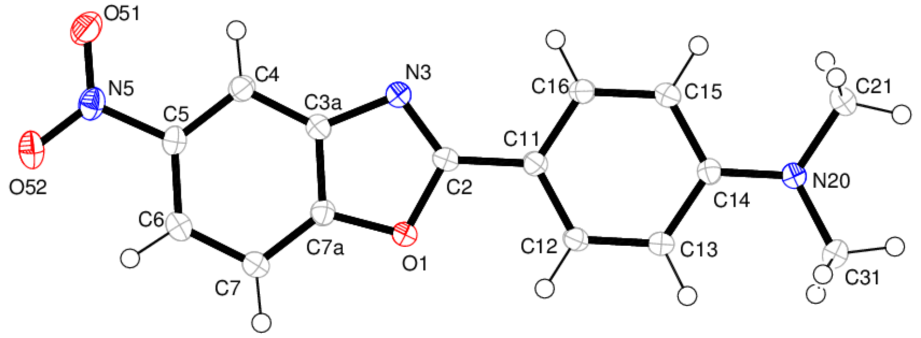

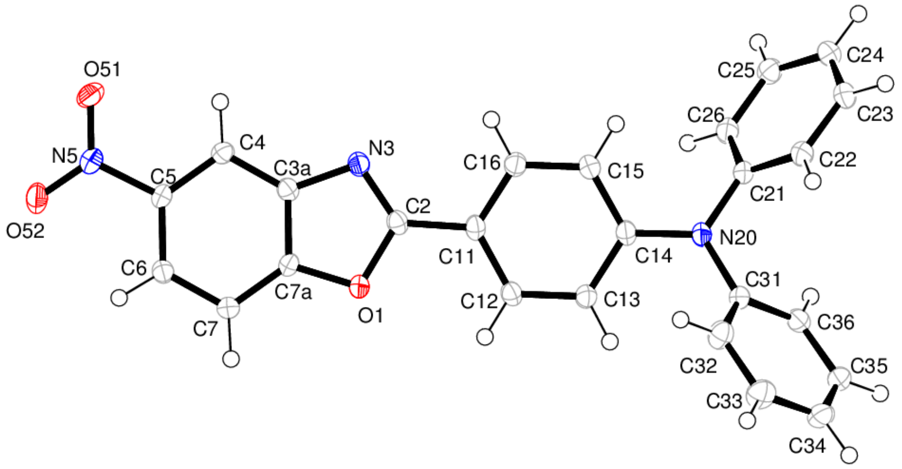

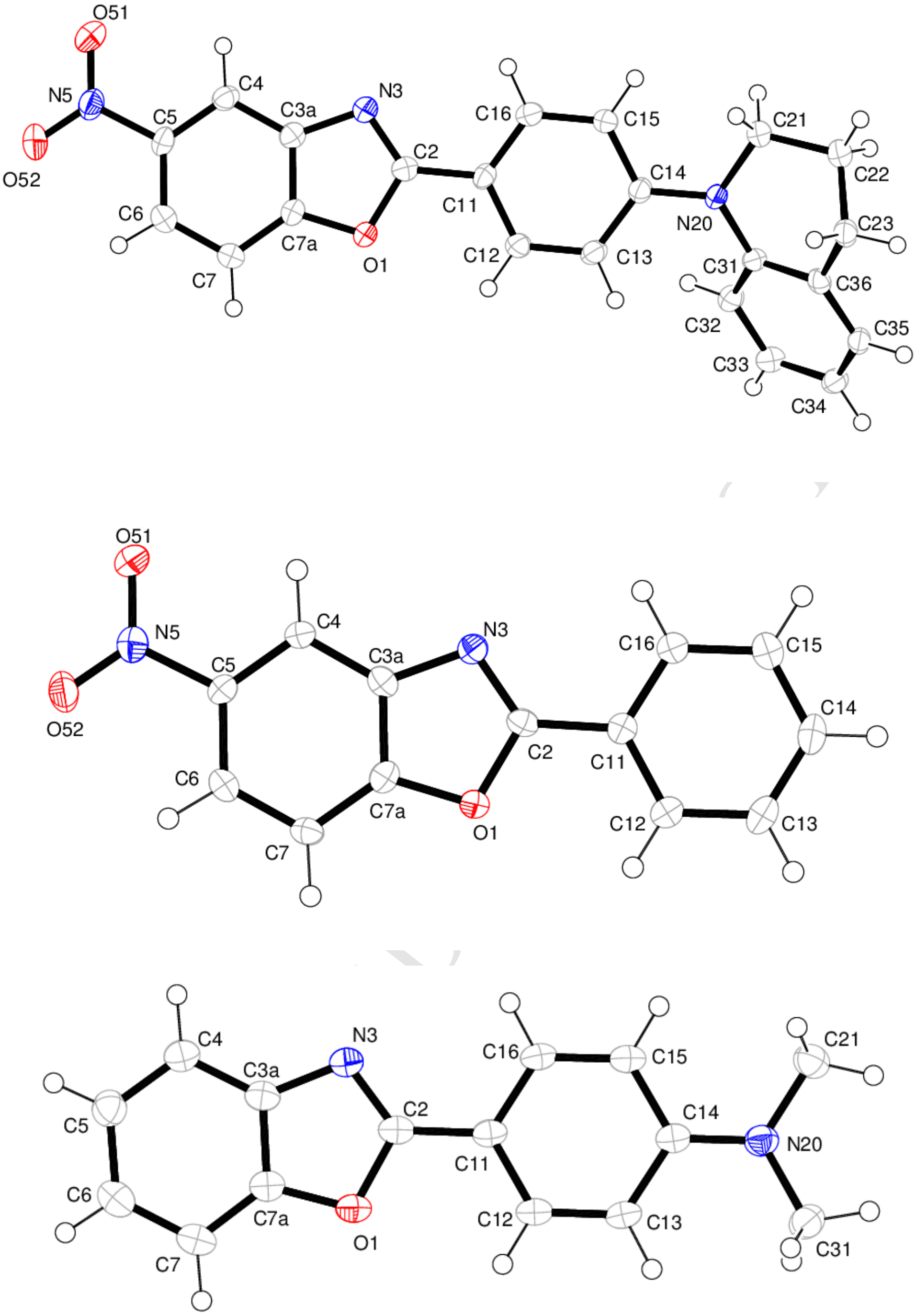

Fig. 2. The shape of molecules for **DMA_LT** (1), **DPA_LT** (2), **THQ_LT** (3), **A_LT** (4) and **D_LT** (5) with the atom numbering scheme. Displacement ellipsoids are drawn at 50% probability level.

Crystal data, intensity measurement conditions and structure refinement details of the compounds are given in Table S1 (see Supplementary Data). The programs used for the crystal structures analyses were working under WinGX environment [57]. SIR92 was used for solving the structures with direct methods [58]. SHELXL2013 was used for the refinement of the structures [59]. ORTEP3 was used in the preparation of molecular graphics [60]. The supplementary materials could be found at CCDC [61].

Selected bond lengths (Å), valence angles (º), torsion angles (º) and dihedral angles (º) for studied molecules correlated with the mean of the appropriate values found in the comparable molecules taken from CCDC are listed in Table S2 (see Supplementary Data). The bond lengths observed in the benzoxazole moiety are very similar in all studied compounds and agree well with those deposited so far in CCDC data base (see references bellow Table S2 in Supplementary Data). The external C(14)-N(20) bond length is significantly influenced by the type of substituents on amine nitrogen atom N(20). The effect depends on conjugation between the lone pair of amine group and π-electron system of phenyl ring, and was also observed for 6-amino-1*H*-pyrazolo[3,4-*b*]quinoline derivatives [62]. The internal valence angles in the oxazole ring match the values from CCDC data base, however those in the benzene ring of benzoxazole moiety are clearly influenced by the nitro group at C(5) [63]. It is worth to emphasize that the dihedral angle between the benzoxazole moiety and phenyl substituent at C(2) is close to 0° in all studied structures, suggesting strong conjugation of those π-systems. The packing of molecules is shown in Fig. S1–S5 (see Supplementary Data). As can be seen from Table S3 (see Supplementary Data) there is no strong or moderate intermolecular interactions in the crystal structures. The geometry found for the molecules in the crystalline state should be also preserved for the molecules in the polymer matrix and thus could be considered as responsible for particular physical properties of the studied non-linear optical materials.

3.2. Non-linear optical studies

Such prepared microcrystalline chromophores were embedded into the liquid oligoetheracrylate (OEA) photopolymers using a method similar to the described earlier [64]. The solidification was performed by 371 nm pulsed nitrogen laser with power density varied up to 400 MW/cm^2 by Glan polarizer. The additional dc-electric field was applied in order to align the chromophores.

Second-order non-linear optical susceptibilities were measured by the Kurtz powder test where a polymer supported the crystalline powder. The Nd: YAG laser operating at 1064 nm and possessing pulses of 12 ns, maximal power 0.95 MW, pulse repetition frequency 13 Hz was applied as the fundamental ones. The exploration of photoinduced changes was performed by a spectrophotometer with 2 nm spectral resolution connected to the CCD camera. This detector registered the 532 nm doubled frequency signal and cut the fluorescence scattering noise. The reference samples were $BiBO_3$ single crystals.

As a consequence, we have determined the effective susceptibility of the polymer/powder compounds. Taking into account the second-order non-linear optical susceptibilities we obtained hyperpolarizability magnitudes. The optimized concentration for the titled molecules was equal to 12 %. The increase of this content favoured aggregation which limit the efficiency of the SHG output.

The microscopic view of such a poled polymer is presented in Fig. 3.

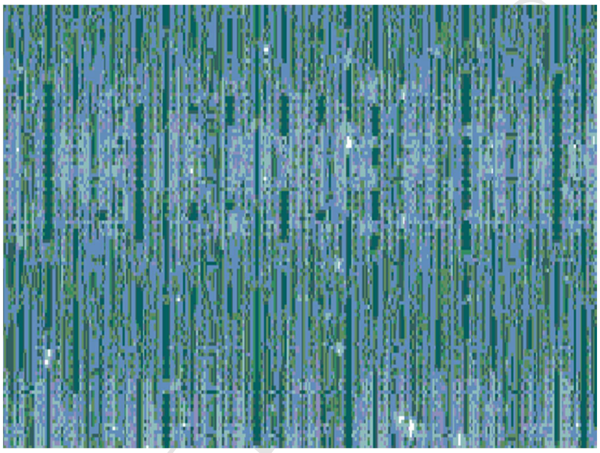

Fig. 3. Microscopic image of the photopolymerized dc-field aligned chromophore (the scale bar size is equal to 100 μm).

The presented composite (Fig. 3) show an existence of the aligned crystallite chromophore. Moreover during the solidification between the chromophore and the polymer there occurs some voids which are responsible for the ability of the chromophore to be oriented in the external dc-electric field.

The performed time kinetics SHG measurements (not presented here) have shown that the most effective SHG output was achieved for the samples **NPA**.

The huge temporary shift of the SHG maxima (29.2 ns) indicates on the occurrence of the trapping levels favouring additional light scattering. The output SHG is very sensitive to the photo solidifying laser beam power density (see Fig. 4) with laser beam diameter about 2.2 mm.

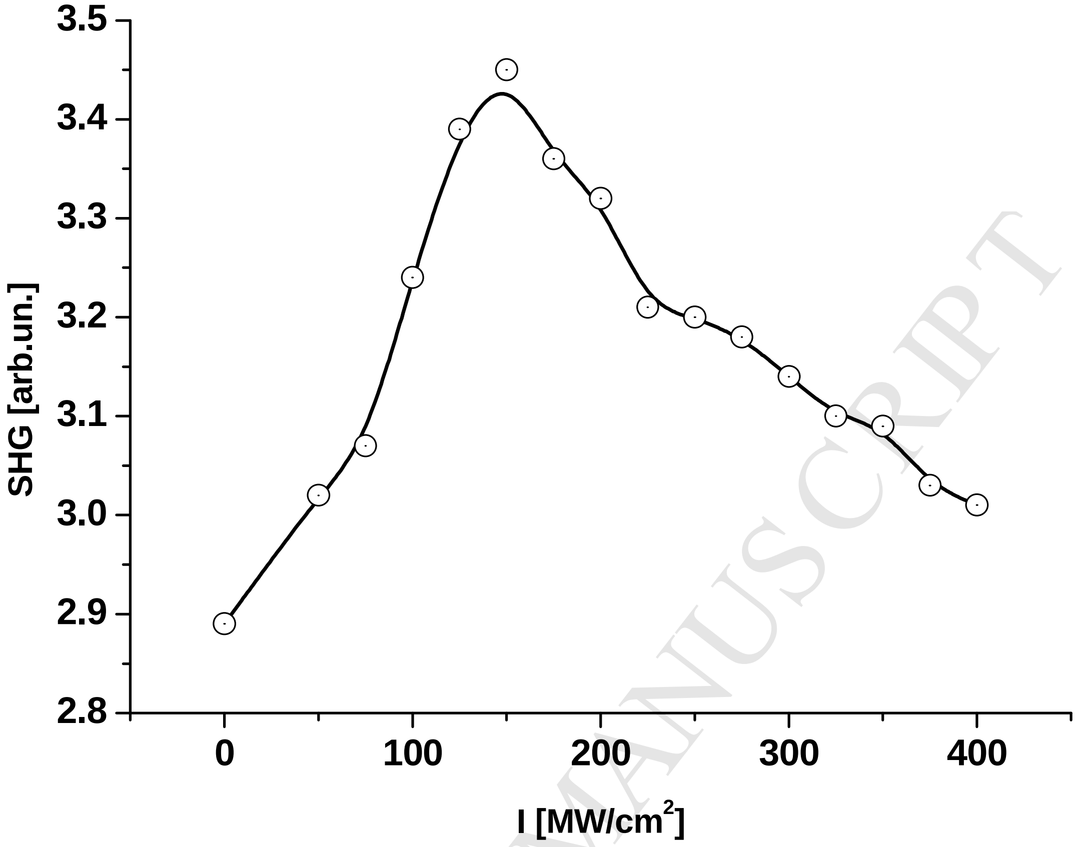

Fig. 4. Dependence of the effective second order susceptibilities versus the applied photoinduced power density.

From Figure 4, one can see that the optimal photo-solidified power density is 180 MW/cm^2. The further decrease is caused by the some cross-linking between the chromophore and the OEA photopolymers, sufficiently suppressing the output SHG.

3.3. Quantum chemical simulations

The electronic parameters for the titled compounds were investigated using Gaussian W09 package [65] at the DFT level [66, 67]. Initial geometries of molecules were estimated by PM6 method and these models were subsequently optimized by DFT B3LYP/6-31 method [68, 69]. The principal parameters of the electronic structure for the titled compounds and the hyper-polarizabilities are presented in the Tables 1, and 2, respectively.

It is clearly seen that maximum second order susceptibility is observed for the **NPA**, and minimum – for **DMA**. For convenience the experimentally determined second order susceptibilities are given in the last row of the Table 1. There is observed an obvious correlation between the calculated second-order hyper-polarizabilities and experimentally measured effective second-order hyper-polarizabilities. Moreover, there is also observed a correlation with the ground state dipole moments.

Table 1. Principal parameters of electronic structure for the titled compounds

	E HOMO, eV	E LUMO, eV	dE, eV	Dipole moment	β (esu)
THQ	-5.308	-2.530	2.778	9.1588	$6.6715 \cdot 10^{-30}$
DPA	-5.416	-2.748	2.668	9.5178	$6.4198 \cdot 10^{-30}$
NPA	-5.429	-2.736	2.693	9.6621	$7.5531 \cdot 10^{-30}$
MPA	-5.520	-2.677	2.843	10.5492	$6.2090 \cdot 10^{-30}$
DMA	-5.521	-2.653	2.868	10.7574	$5.3118 \cdot 10^{-30}$

Table 2. Values of the hyperpolarizabilities calculated theoretically (in esu) and compared with the experimentally measured second order susceptibilities in pm/V at wavelength 1064 nm (in brackets).

	DMA	**DPA**	**MPA**	**NPA**	**THQ**
β_{xxx}	-609.3187	-725.8475	-697.4138	-780.3962	744.5081
β_{xyy}	-23.9171	-46.8246	-24.9234	-62.8461	16.178
β_{xzz}	22.1679	14.833	8.6417	-10.7969	-28.3037
β_{yyy}	15.5131	-8.1277	-0.8136	25.7757	3.8524
β_{xxy}	55.3835	-124.3877	-70.1013	164.9506	55.8662
β_{yzz}	-2.8579	-1.3703	-2.9697	-11.2767	4.3444
β_{zzz}	0.0031	1.9806	3.0718	-4.5096	6.5477
β_{xxz}	-0.0033	-58.1248	-46.1329	54.3306	103.0043
β_{yyz}	0.0021	-7.8128	1.8660	2.7321	-1.4015
β_{xyz}	0.0011	1.0092	11.3957	-1.5537	-9.8352
β_x	-611.0679	-757.8391	-713.6955	-854.0392	732.3824
β_y	68.0387	-133.8857	-73.8846	179.4496	64.063
β_z	0.0019	-63.957	-41.1951	52.5531	108.1505
β(esu) d_{eff}	$5.3118 \cdot 10^{-30}$	$6.6715 \cdot 10^{-30}$	$6.2090 \cdot 10^{-30}$	$7.5531 \cdot 10^{-30}$	$6.4198 \cdot 10^{-30}$
d_{eff} (1064 nm)	(0.56 pm/V)	(1.67 pm/V)	(1.06 pm/V)	(2.1 pm/V)	(1.49 pm/V)

The principal space distributions of the HOMO and LUMO molecular orbital levels are presented in Fig. 5.

DMA HOMO

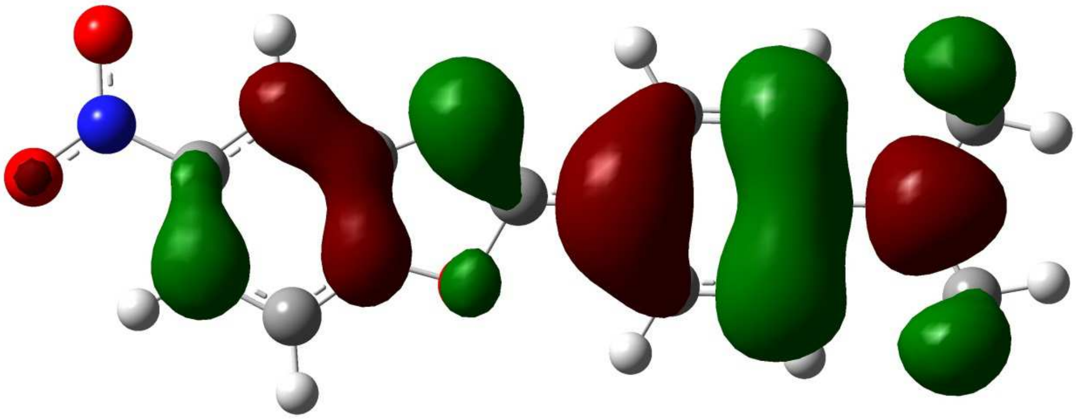

DMA LUMO

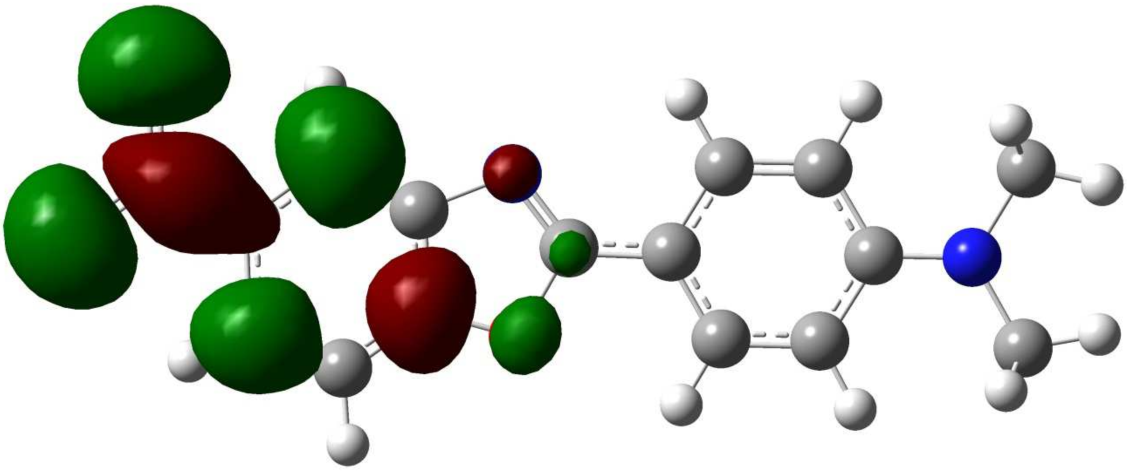

DPA HOMO

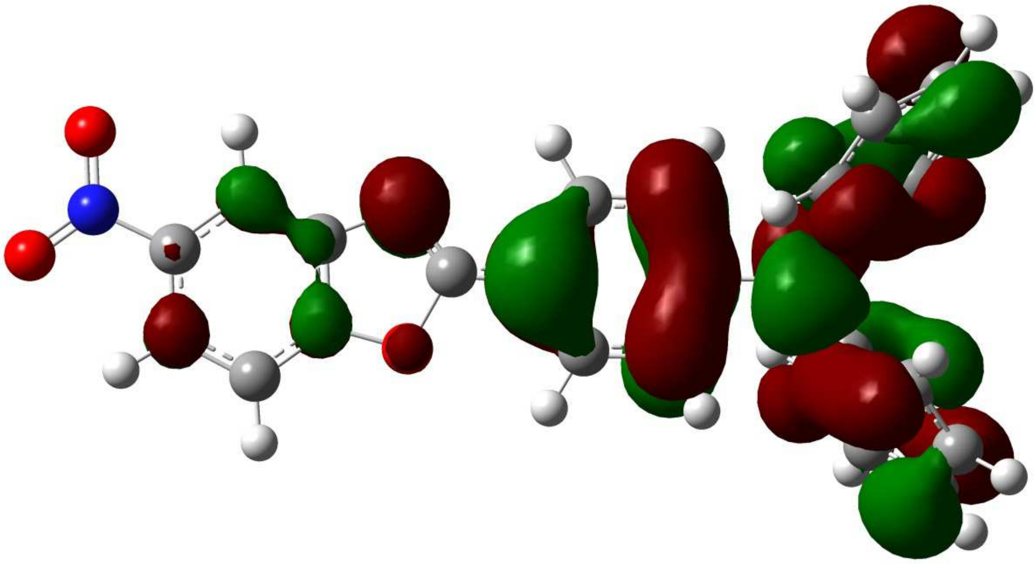

DPA LUMO

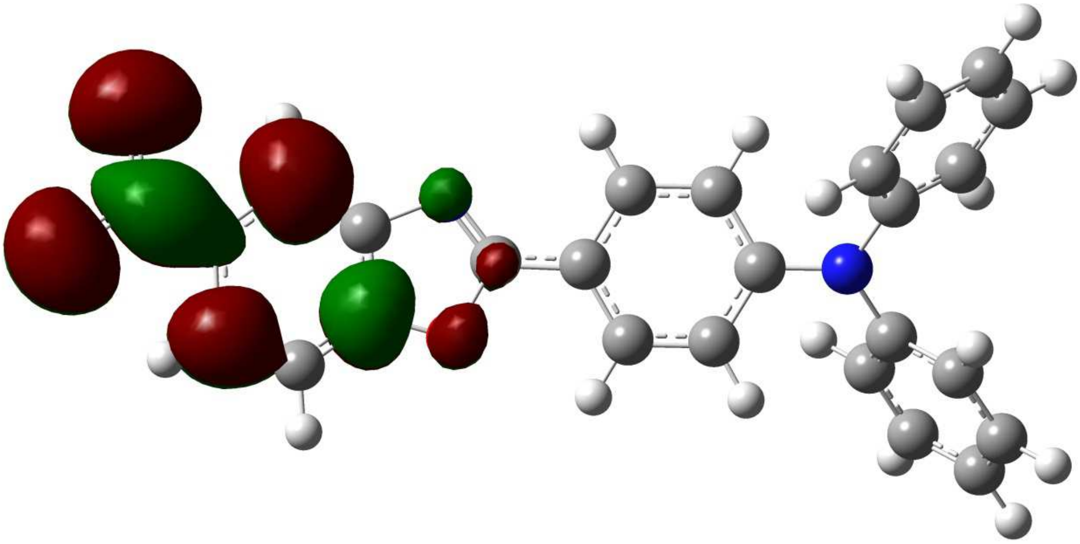

MPA HOMO

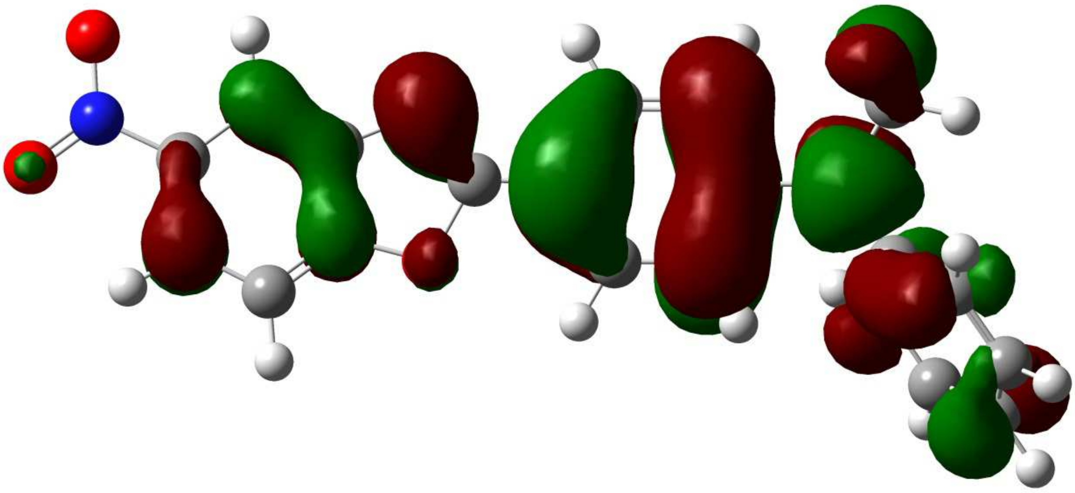

MPA LUMO

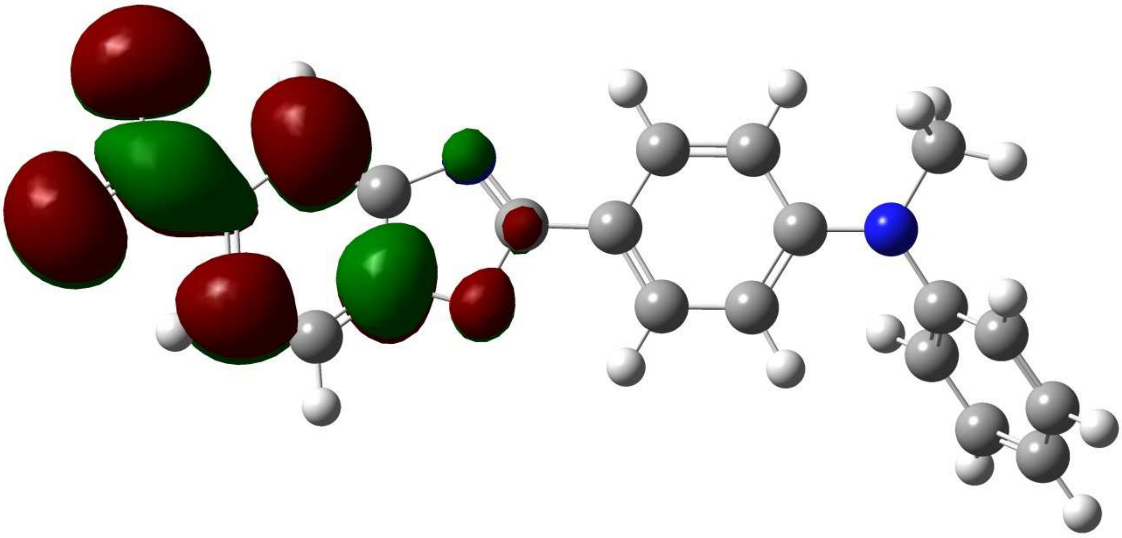

NPA HOMO

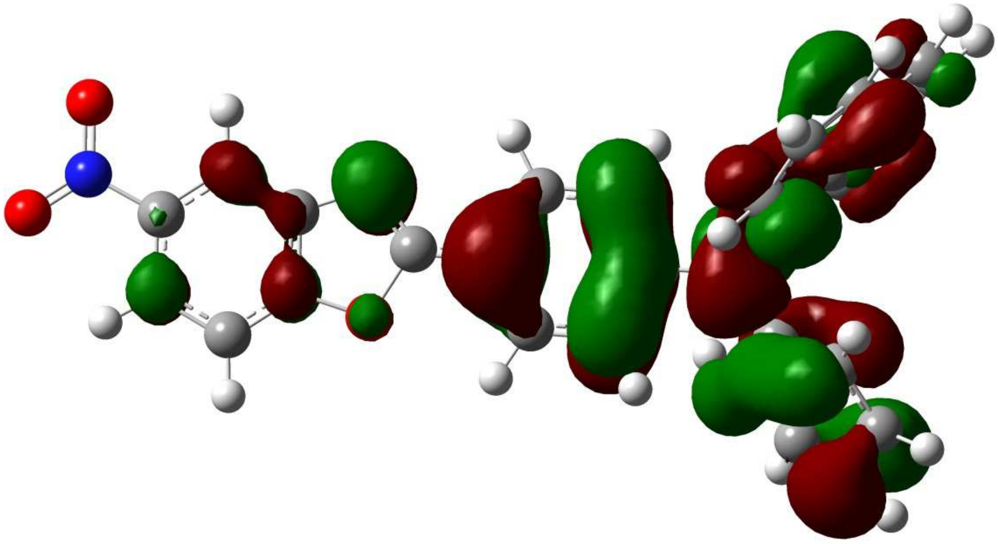

NPA LUMO

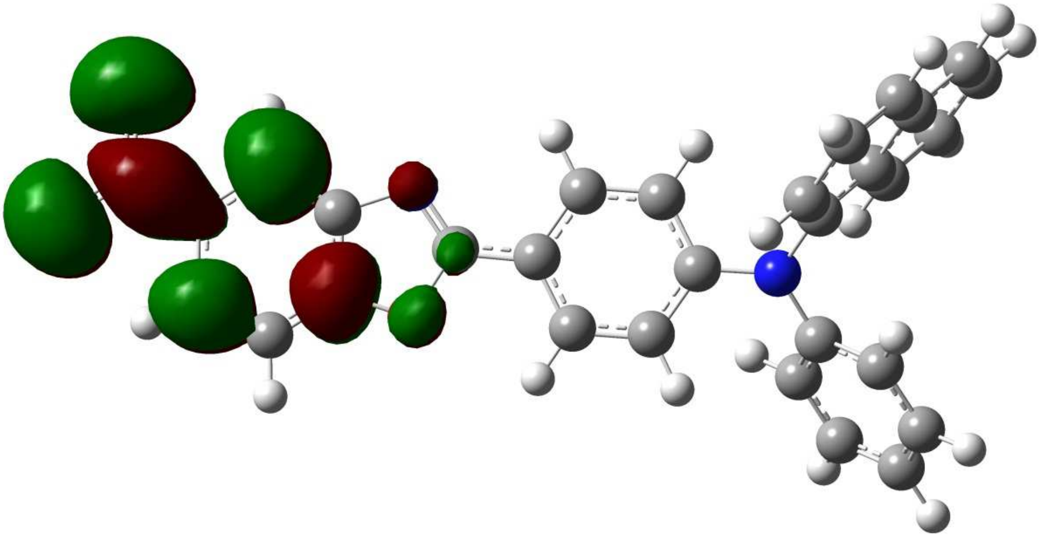

THQ HOMO

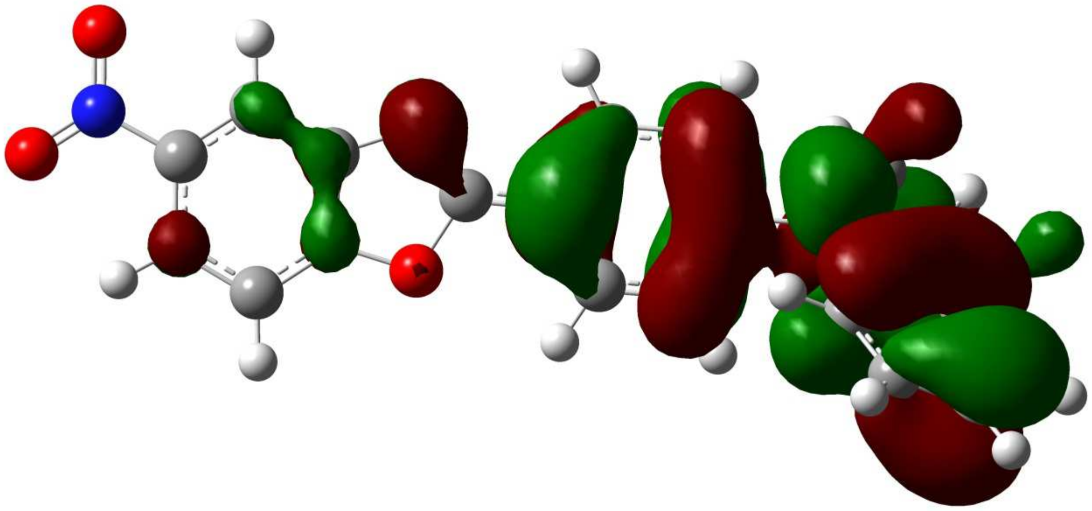

THQ LUMO

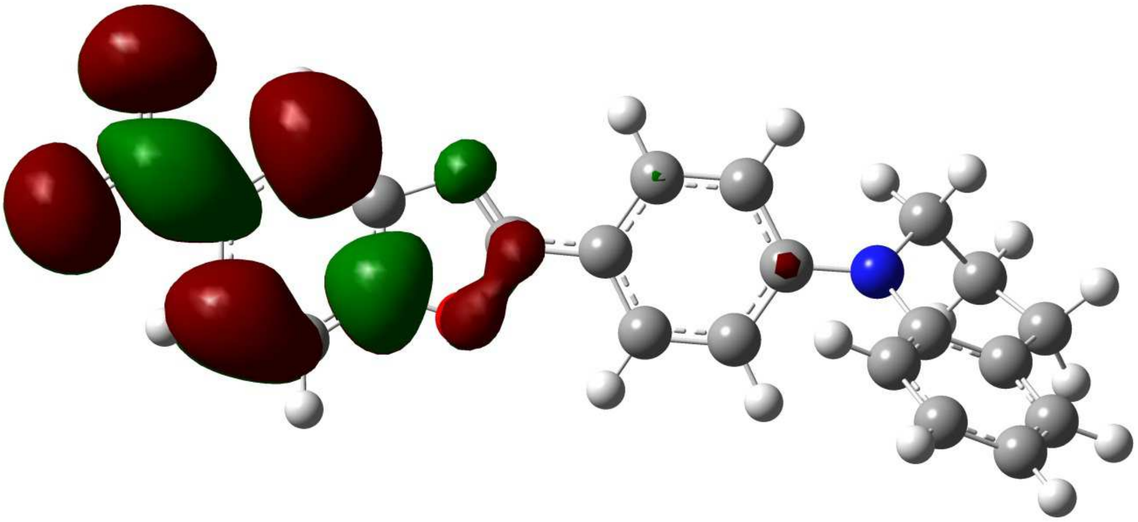

Fig. 5. Space distribution of the HOMO and LUMO molecular orbitals.

This figure unambiguously confirms an existence of charge transfer between the donor-acceptor groups. The space separation between these groups may be a consequence of the different polarizabilities of the donor and acceptor groups determining the charge transfer. The π-conjugated bonds play here crucial role, however the energy positions of the LUMO also play substantial role.

Following the approach described previously [6,7,70,71], the fundamental limit for resonance effective second-order optical hyperpolarizability β is equal to 57 × 10^{-28} esu. This is obtained by taking into account of the influence of polymer. However, the effective hyperpolarizabilities evaluated from the experimental SHG time kinetics curves were varied from 7,31 × 10^{-30} to 8,7 × 10^{-30} esu. This fact principally agreed with the intrinsic hyperpolarizabilities determined by the ratio between the measured and the fundamental limits of the mentioned model equal to about 0.013, which is comparable with the other organic molecules [4]. Without the dc-field, one can observe decrease of the susceptibility up to 40–50 % with respect to that maximally achieved.

This fact shows more efficient properties of the titled chromophores with respect to other organic NLO chromophores including those possessing larger π-conjugated chains and the d-localized states [71–75].

3.4. *Electrochemical studies and UV-Vis absorption spectra – experimental HOMO-LUMO energy levels*

In order to determine the experimental HOMO energy levels, the electrochemical oxidation potentials were examined by means of cyclic voltammetry (CV) and confirmed by independent measurements of differential pulse voltammetry (DPV). The oxidation part of cyclic voltammograms of studied benzoxazoles: **DMA**, **MPA**, **DPA**, **NPA** and **THQ**, together with ferrocene, are depicted in **Figure S6** (see Supplementary Data). The investigated benzoxazoles exhibit reversible oxidation peaks (excluding **THQ**, for which reversal peak is very weak) at the platinum electrode with reference to non-aqueous reference electrode (Ag/Ag^+, calibrated with ferrocene/ferrocenium redox couple).

According to the Koopmans' theorem the energy of the HOMO is a good approximation to the negative experimental ionization potential ($-IP$). Ionization potentials were calculated as follows: $-IP = E_{HOMO} = -(1.4 \pm 0.1) \times (qV_{CV}) - (4.6 \pm 0.08)$ eV where: q – electron charge in ē, $V_{CV} = E_{ox}$ – the first oxidation potential obtained from CV measurements in V) [76]. LUMO energy levels were determined from the following equation: LUMO = $-(IP + E_{00})$, where E_{00} – optical energy gap evaluated from the onset of the first absorption band of the compounds in dichloromethane solution (the spectra are depicted in Figure 6).

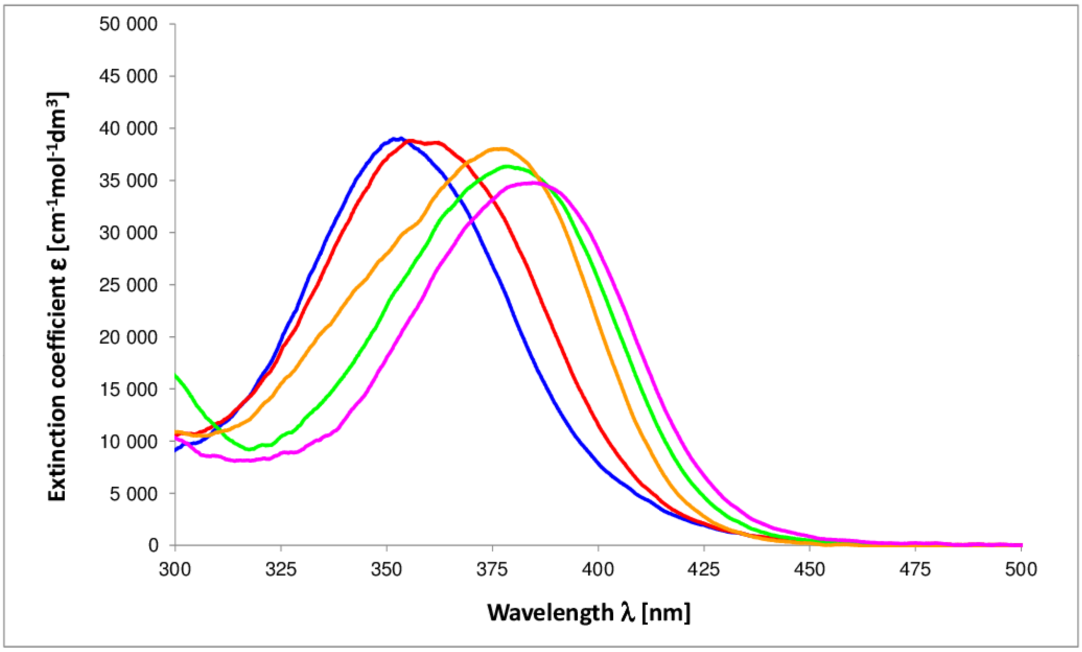

Figure 6. Absorption spectra for studied molecules (**DMA**, blue; **MPA**, red; **DPA**, green, **NPA**, orange and **THQ**, pink), recorded in dichloromethane solutions.

The values of oxidation potentials, optical energy gaps and HOMO/LUMO energy levels are given in Table 3.

Table 3. Oxidation potentials, energy gaps, HOMO and LUMO energy levels for studied molecules.

	$E_{ox/ferrocene}$ [eV]	HOMO [eV]	E_{gap} [eV]	LUMO [eV]
DMA	0.612	-5.457	3.069	-2.388
MPA	0.610	-5.454	3.019	-2.435
DPA	0.656	-5.518	2.921	-2.597
NPA	0.650	-5.510	2.964	-2.546
THQ	0.470	-5.258	2.897	-2.361

The HOMO energy levels agree quite well with those predicted by DFT calculations (see Table 1). Calculated E_{gap} and, in consequence, LUMO levels, seem to be underestimated. However, one has to remember that calculated HOMO and LUMO energy levels could vary depending on the chosen functional [77]. In addition, DFT methodology leads to problems of accurate approximation of energy gap in push-pull molecules with possible rotations of donor group [78]. Finally there exists some influence of surrounding polymer which changes the output susceptibilities [79–81].

5. Conclusions

In summary, we have shown a possibility to use the substituted 4-(5-nitro-1,3-benzoxazol-2-yl)aniline) chromophores embedded into the photopolymer matrices for the optically operated second harmonic generation. It is shown that varying the effective external fields' one can operated by the output NLO parameters. The appropriate variation of the backside donor group allows effectively operated by second order susceptibilities. More importantly, varying the UV-induced power at 371 nm, one can operate by the photo-solidified power for operation by the effective second order susceptibilities. The DFT simulations confirm the principal role of the donor–acceptor intra-chromophore charge transfer in the observed output second-order efficiencies. However, some role is played by external fields. The effects are crucially dependent on the photoillumination time.

ACKNOWLEDGMENTS

The authors would like to thank, for purchasing part of the equipment used in the research, to European Regional Development Fund within the Polish Innovation Economy Operational Program (contract no. POIG.02.01.00-12-023/08). This research was also partly financed by the Ministry of Science and Higher Education of the Republic of Poland basic funding for University of Agriculture (DS 3133/2016). The project was also financially supported by King Saud University, Vice Deanship of research chairs.

References

[1] Wu W, Qin J, Li Z. New design strategies for second-order nonlinear optical polymers and dendrimers. Polymer 2013;54:4351-82.

[2] Sudhahar S, Krishna Kumar M, Silambarasan A, Muralidharan R, Mohan Kumar R. Studies on Structural, Spectral, and Optical Properties of Organic Nonlinear Optical Single Crystal: 2-Amino-4,6-dimethylpyrimidinium p-Hydroxybenzoate. J Mater 2013;2013:articleID:539312 (7 pp).

[3] Liu J, Xu G, Liu F, Kityk I, Liu X, Zhen Z. Recent advances in polymer electro-optic modulators. RSC Advances 2015;5:15784-94.

[4] Kolev Ts, Kityk IV, Ebothe J, Sahraoui B. Intrinsic hyperpolarizability of 3-dicyanomethylene-5,5-dimethyl-1-[2-(4-hydroxyphenyl)ethenyl]-cyclohexene nanocrystallites incorporated into the photopolymer matrices. Chem Phys Lett 2007;443:309-12.

[5] Larry R. Dalton, Xu Chengzeng, Wu Bo, Aaron W. Harper. Frontiers of Polymers and Advanced Materials, pp 175–185 Techniques for Ultrastructure Synthesis: Preparation of Second Order Nonlinear Optical Materials. Springer, 1994.

[6] Kuzyk MG. Fundamental limits of All nonlinear-optical phenomena that are representable by a second-order nonlinear susceptibility. J Chem Phys 2006;125:154108(10 pp).

[7] Moreno JP, Kuzyk MG. Fundamental limits of the dispersion of the two-photon absorption cross section. J Chem Phys 2005;123:194101(13 pp).

[8] Kuzyk MG, Dirk CW. Characterization Techniques and Tabulations for Organic Nonlinear Optical Materials, Marcel Dekker, New York, 1998.

[9] Senthil K, Kalainathan S, Hamada F, Kondo Y. Bulk crystal growth and Nonlinear optical characterization of stilbazolium derivative crystal: 4-[2-(3,4-Dimethoxyphenyl) ethenyl]-1 methyl pyridinium tetraphenylborate (DSTPB) for NLO device fabrications. RSC Adv 2015;5:79298-308.

[10] Wu W, Wang Z, Xiao R, Xu Z, Li Z. Main chain dendronized hyperbranched polymers: convenient synthesis and good second-order nonlinear optical performance. Polym Chem 2015;6:4396-403.

[11] Yalçın E, Achelle S, Bayrak Y, Seferoğlu N, Barsella A, Seferoğlu Z. Styryl-based NLO chromophores: synthesis, spectroscopic properties, and theoretical calculations. Tetrahedron Lett 2015;56:2586-9.

[12] Bureš F, Cvejn D, Melánová K, Beneš L, Svoboda J, Zima V, et al. Effect of intercalation and chromophore arrangement on the linear and nonlinear optical properties of model aminopyridine push-pull molecules. J Mat Chem C 2016;4:468-78.

[13] Spiridon MC, Iliopoulos K, Jerca FA, Jerca VV, Vuluga DM, Vasilescu DS, et al. Novel pendant azobenzen/polymer systems for second harmonic generation and data storage. Dyes and Pigments 2015;114:24-32.

[14] Zhang H, Liao Q, Wang X, Xu Z, Fu H. Self-assembled organic hexagonal micro-prisms with high second harmonic generation efficiency for photonic devices. Nanoscale 2015;7:10186-92.

[15] Cidália M, Castro R, Belsley M, Raposo MMM. Push-pull second harmonic generation chromophores Bering pyrrole and triazole heterocycles functionalized with several acceptor moieties: Syntheses and characterization. Dyes and Pigments 2016;128:89-95.

[16] Gao J-X, Xiong J-B, Xu Q, Tan Y-H, Liu Y, Wen H-R, et al. Supramolecular Interactions Induced Chirality Transmission, Second Harmonic Generation Responses, and Photoluminescent Property of a Pair of Enantiomers from In Situ [2 + 3] Cycloaddition Synthesis. Cryst Growth Des 2016;16:1559-64.

[17] Tang R, Zhou S, Xiang W, Xie Y, Chen H, Peng Q, et al. New ”X-type” second-order nonlinear optical (NLO) dendrimers: fewer chromophore moieties and high NLO effects. J Mater Chem C 2015;3:4545-52.

[18] Ziemann EA, Mietner JB, Deffner M, Van Steerteghem N, Clays K, Herrmann C, et al. Extended Threefold-Symmetric Second-Harmonic-Generation Chromophores Based on 1,3,5-Trisubstituted Benzene Complexes. Eur J Inorg Chem 2015:4244-53.

[19] Toury T, Zyss J, Chernyak V, Mukamel S. Collective Electronic Oscillators for Second-Order Polarizabilities of Push-Pull Carotenoids. J Phys Chem A 2001;105:5692-703.

[20] Messier J, Kajzar F, Prasad P, Williams DJ. Introduction to Nonlinear Optical Effects in Molecules & Polymers, John Wiley & Sons, New York, 1991.

[21] Kuzyk MG. Using fundamental principles to understand and optimize nonlinear-optical materials. J Mater Chem 2009;19:7444-65.

[22] Kuzyk MG. Physical Limits on Electronic Nonlinear Molecular Susceptibilities. Phys Rev Lett 2000;85:1218-21.

[23] Zhao J, Chillara VK, Ren B, Cho H, Qiu J, Lissenden CJ. Second harmonic generation In composites: Theoretical and numerical analyses. J App Phys 2016;119:064902(14 pp).

[24] Shen YR. Basic Theory of Surface Sum-Frequency Generation. J Phys Chem C 2012;116:15505-9.

[25] Zyss J. Molecular Nonlinear Optics; Materials, Physics, and Devices. Academic Press, Inc. 1994.

[26] Kuzyk MG, Singer KD, Stegeman GI. Theory of Molecular Nonlinear Optics. Adv Opt Photon 2013;5:4-82.

[27] Vampa G, McDonald CR, Orlando G, Corkum PB, Brabec T. Semiclassical analysis of high harmonic generation in bulk crystals. Phys Rev B 2015;91:064302(11 pp).

[28] Qian J. Zhu Z, Qin A, Qin W, Chu L, Cai F, et al. High-Order Non-linear Optical Effects In Organic Luminogens with Aggregation-Induced Emission. Adv Mater 2015;27:2332-9.

[29] Watkins DS, Kuzyk MG. The effect of electron interactions on the universal properties of systems with optimized off-resonant intrinsic hyperpolarizability. J Chem Phys 2011;134:094109(10 pp).

[30] Beels MT, Biaggio I, Reekie T, Chiu M, Diederich F. Two-photon absorption and spectroscopy of the lowest two-photon transition In small donor-acceptor-substituted organic molecules. Phys Rev A 2015;91:043818(14 pp).

[31] Bruno V, Castaldo A, Centore R, Sirigu A, Sarcinelli F, Casalboni M, et al. Second Harmonic Generation in Polymers Containing a New Azo Chromophore Based on Phenylnitrobenzoxazole. J Polym Sci Part A: Polym Chem 2002;40:1468-75.

[32] Persico P, Centore R, Sirigu A, Casalboni M, Quatela A, Sarcinelli F. Synthesis and Nonlinear Optical Properties of Methacrylate Polymers Based on 2-[4-(N-Methyl,N-hydroxyethylamino)phenylazo]-phenyl-6-nitrobenzoxazole Chromophore. J Polym Sci Part A: Polym Chem 2003;41:1841-7.

[33] Beltrani T, Bösch M, Centore R, Concilio S, Günter P, Sirigu A. Nonlinear optical properties of polymers containing a new azophenylbenzoxazole chromophore. Polymer 2001;42: 4025-9.

[34] Hwang J, Moon H, Seo J, Park SY, Aoyama T, Wada T, et al. Synthesis and characterization of photoconducting non-linear optical polymers containing indole-benzoxazole moiety. Polymer 2001;42:3023-31.

[35] Park KH, Yeon KM, Lee MY, Lee S-D, Shin D-H, Lee CJ, et al. Synthesis and nonlinear optical properties of PMMA copolymers having novel benzoxazole chromophores attached with various electron-withdrawing groups. Polymer 1998;26: 7061-6.

[36] Park KH, Kwak MG, Jahng WS, Lee CJ, Kim N. Nonlinear optical polymers with novel benzoxazole chromophores III. Synthesis and characterization of self-crosslinkable glycidyl methacrylate copolymers. React Funct Polym 1999;40:41-9.

[37] Hwang J, Sohn J, Park SY. Synthesis and Structural Effect of Multifunctional Photorefractive Polymers Containing Monolithic Chromophores. Macromolecules 2003;36:7970-6.

[38] Santos FS, Costa TMH, Stefani V, Gonçalves PFB, Descalzo RR, Benvenutti EV et al. Synthesis, Characterization, and Spectroscopic Investigation of Benzoxazole Conjugated Schiff Bases. J Phys Chem A 2011;115:13390-8.

[39] Hillebrand S, Segala M, Buckup T, Correia RRB, Horowitz F, Stefani V. First hyperpolarizability in proton-transfer benzoxazoles: computer-aided design, synthesis and study of a new model compound. Chem Phys 2001;273:1-10.

[40] Castaldo A, Centore R, Peluso A, Sirigu A, Tuzi A. Structure and Electronic Properties of Extended Chromophores for Applications in Second-Order Nonlinear Optics. Struct Chem 2002;13:27-36.

[41] Yadav UN, Kumbhar HS, Deshpande SS, Sahoo SK, Shankarling GS. Photophysical and thermal properties of novel solid state fluorescent benzoxazole based styryl dyes from a DFT study. RSC Advances 2015;5:42971-7.

[42] Wang C-S, Wang I-W, Cheng K-L, Lai CK. The effect of polar substituents on the heterocyclic benzoxazoles. Tetrahedron 2006;62:9383-92.

[43] Jin X, Cui Y, Gao J, Nie J, Liu W, Qian G. High thermally stable hybrid nonlinear optical films containing heterocycle chromophores. Thin Solid Films 2009;517:5079-83.

[44] Zeyrek CT, Ünver H, Arpacı OT, Polat K, İskeleli NO, Yildiz M. Experimental and theoretical characterization of the 2-(4-bromobenzyl)-5-ethylsulphonyl-1,3-benzoxazole. J Mol Struct 2015;1081:22-37.

[45] Zhang N, Liu D, Zhang H, Yu J, Wu Z, Zhu Q, et al. Cadmium (II) Supramolecular complexes constructed from phenylbenzoxazole-based ligand: self-assembly, structural features and nonlinear optical properties. RSC Adv 2016;6:86158-64.

[46] Mary YS, Al-Shehri MM, Jalaja K, Al-Omary FAM, El-Emam AA, Panicker Y, et al. Synthesis, vibrational spectroscopic investigations, molecular docking, antibacterial studies and molecular dynamics study of 5-[(4-nitrophenyl)acetamido]-2-(4-tert-butylphenyl)benzoxazole. J Mol Struct 2017;1133:557-73.

[47] Mervinskii RI, Petrenko OG, Kityk IV, Lazarenko ET. Relief molding in the layer of a liquid photopolymerizing composition taking into account optical spectral characteristics of the transition layer. Opt Spectrosc 1995;78**:**287-91.

[48] Kulhánek J, Bureš F, Wojciechowski A, Makowska-Janusik M, Gondek E, Kityk IV. Optical Operation by Chromophores Featuring 4,5-Dicyanoimidazole Embedded within Poly(methyl methacrylate) Matrices. J Phys Chem A 2010;114*:*9440-6.

[49] CrysAlisPro, Oxford Diffraction Ltd., Version 1.171.33.66.

[50] Nonius, COLLECT, Nonius, Delft, The Netherlands, 1997–2000.

[51] Otwinowski Z, Minor W. Macromolecular crystallography, Part A, in: C.W. Carter Jr., R.M. Sweet (Eds.), Methods in Enzymology, vol. 276, Academic Press, New York, 1997, p.307.

[52] So Y-H, Heeschen JP. Mechanism of Polyphosphoric Acid and Phosphorus Pentoxide-Methanosulfonic Acid as Synthetic Reagents for Benzoxazole Formation. J Org Chem 1997;62:3552-61.

[53] Surry DS, Buchwald SL. Biaryl Phosphane Ligands in Palladium-Catalyzed Amination. Angew Chem Int Ed Eng 2008;47:6338-61.

[54] Xie H-Z, Gao Q, Liang Y, Wang H-S, Pan Y-M. Palladium-catalyzed synthesis of benzoxazoles by the cleavage reaction of carbon-carbon triple bonds with *o*-aminophenol. Green Chem 2014;16:2132-5.

[55] Bhagyasree JB, Varghese HT, Panicker CY, Samuel J, Van Alsenoy C, Ertan-Bolelli T, et al. Quantum mechanical and spectroscopic (FT-IR, FT-Raman, ^{1}H-NMR and UV) investigations of 5-nitro-2-phenylbenzoxazole. J Mol Struct 2014;1063:16-29.

[56] Kawashita Y, Nakamichi N, Kawabata H, Hayashi M. Direct and Practical Synthesis of 2-Arylbenzoxazoles Promoted by Activated Carbon. Org Lett 2003;5:3713-5.

[57] Farrugia LJ. *WinGX* and *ORTEP for Windows*: an update. J Appl Cryst 2012;45: 849-54.

[58] Altomare A, Cascarano G, Giacovazzo C, Guagliardi A, Burla MC, Polidori G, et al. SIR92 – a program for automatic solution of crystal structures by direct methods. J Appl Cryst 1994;27:435.

[59] Sheldrick GM. A short history of *SHELX*. Acta Cryst 2008;A64:112.

[60] Farrugia LJ. *ORTEP*-3 for Windows – a version of *ORTEP*-III with a graphical user interface (GUI). J Appl Cryst 1997;30:565.

[61] Crystallographic data (structure factors excluded) for structures reported herein have been deposited in Cambridge Crystallographic Data Centre as supplementary publication no CSD-1486178 for **A_RT**, -1486179 for **A_LT**, -1486180 for **D_RT**, -1486181 for **D_LT**, -1486182 for **DMA_RT**, -1486183 for **DMA_LT**, -1486184 for **DPA_LT** and -1486185 for **THQ_LT**. Copies of these data can be obtained on

application to: CCDC, 12 Union Road, Cambridge CB2 1EZ, UK [Fax: (internat.) +44-1223/336-033, E-mail: deposit@ccdc.cam.ac.uk] (free of charge).

[62] Uchacz T, Szlachcic P, Wojtasik K, Mac M, Stadnicka K. Amino derivatives of 1,3-diphenyl-1*H*-pyrazolo[3,4-*b*]quinoline – Photophysics and implementation of molecular logic switches. Dyes and Pigments 2016;124:277-92.

[63] Domenicano A, Murray-Rust P. Geometrical substituent parameters for benzene derivatives: inductive and resonance effects. Tetrahedron Lett. 1979;20:2283-6.

[64] Kityk IV, Mervinskii RI, Kasperczyk J, Jossi S. Synthesis and properties of nm-sized $Sn_2P_2Se_6$ single crystals embedded in photopolymeric host. Mater Lett 1996;27:233-7.

[65] Frisch MJ, Trucks GW, Schlegel HB, Scuseria GE, Robb MA, Cheeseman JR, et al. Gaussian 09, Revision A.1, Gaussian, Inc., Wallingford, CT; 2009.

[66] Parr RG, Yang W. Density-Functional Theory of Atoms and Molecules, Oxford University Press, New York, 1989.

[67] Koch W, Holthausen MC. A Chemist’s Guide to Density Functional Theory, Weinheim, Wiley-VCH, 2000.

[68] Becke AD. Density-functional exchange energy approximation with correct asymptotic behaviour. Phys Rev A 1988;38:3098–100.

[69] Lee C, Yang W, Parr RG. Development of the Colle-Salvetti correlation-energy formula into a functional of the electron density. Phys Rev B 1988;37:785-89.

[70] Kuzyk MG. Fundamental limits on third-order molecular susceptibilities. Opt Lett 2000;25:1183-5.

[71] Kuzyk MG. Fundamental limits on two-photon absorption cross sections. J Chem Phys 2003;119:8327-34.

[72] Bureš F, Čermáková H, Kulhánek J, Ludwig M, Kuznik W, Kityk IV, et al. Structure-Property Relationships and Nonlinear Optical Effects in Donor-Substituted Dicyanopyrazine-Derived Push-Pull Chromophores with Enlarged and Varied π-Linkers. Eur J Org Chem 2012;2012:529-38.

[73] Kulhánek J, Bureš F, Kuznik W, Kityk IV, Mikysek T, Růžička A. Ferrocene-Donor and 4,5-Dicyanoimidazole-Acceptor Moieties In Charge-Transfer Chromophores with π Linkers Tailored for Second-Order Nonlinear Optics. Chem Asian J 2013;8:465-75.

[74] Czerwieniec R, El-Naggar AM, Albassam AA, Kityk IV, Graf M, Yersin H. Electric-field induced nonlinear optical materials based on a bipolar copper (I) complex embedded in polymer matrices. J Mater Sci: Mater Electron 2015;26:8394-7.

[75] Kamanina NV, Serov SV, Shurpo NA, Likhomonova SV, Timonin DN, Kuzhakov PV, et al. Polyimide-fullerene nanostructured materials for nonlinear optics and solar energy applications. J Mater Sci: Mater Electron 2012;23:1538-42.

[76] D’Andrade BW, Datta S, Forrest SR, Djurovich P, Polikarpov E, Thompson ME. Relationship between the ionization and oxidation potentials of molecular organic semiconductor. Org Electron 2005;6:11-20.

[77] Zhang G, Musgrave CB. Comparison of DFT Methods for Molecular Orbital Eigenvalue Calculations. J Phys Chem A 2007;111:1554-61.

[78] Wiggins P, Williams JAG, Tozer DJ. Excited state surfaces in density functional theory: a New twist on an old problem. J Chem Phys 2009;131:091101(4 pp).

[79] Liu J, Xu G, Liu F, Kityk IV, Liu X, Zhen Z. Recent advances in polymer electro-optic modulators. RSC Adv 2015;5:15784-94.

[80] Kuznik W, Rakus P, Ozga K, Parasyuk OV, Fedorchuk AO, Piskach LV, Krymus A, Kityk IV. Laser-induced piezoelectricity in $AgGaGe_{3-x}Si_xSe_8$ chalcogenide single crystals. Eur Phys J Appl Phys 2015;70: 30501.

[81] Reshak AH, Kamarudin H, Kityk IV, Auluck S. Dispersion of Linear, Nonlinear Optical Susceptibilities and Hyperpolarizability of $C_{11}H_8N_2O$ ((-Methoxydicyaqnovinylbenzezne) Crystals. J Phys Chem B 2012;116:13338-43.

Research Highlights

- Second order nonlinear optical susceptibilities of organic chromophores/photopolymer matrices were studied.
- Microscopic hyper-polarizabilities were obtained within the B3LYP DFT approach.
- SHG efficiency versus the photoinduced laser power density is presented.
- DFT simulations confirm the donor–acceptor charge transfer in the observed output second-order efficiencies.
- The effects are crucially dependent on the photo-illumination time.